Unconventional Quantum Phase Transition in a Ring-Exchange Antiferromagnet

Valeri N. Kotov, D. X. Yao, A. H. Castro Neto, and D. K. Campbell

Department of Physics, Boston University, 590 Commonwealth Avenue, Boston, MA 02215

We study the S=1/2 Heisenberg antiferromagnet on a square lattice with nearest-neighbor and plaquette ring exchanges; this model undergoes a quantum phase transition from a spontaneously dimerized phase to Néel order at a critical coupling. We show that as the critical point is approached from the dimerized side the system exhibits strong fluctuations in the dimer background, reflected in the presence of a low-energy singlet mode, with a simultaneous rise in the triplet quasiparticle density. We find that both singlet and triplet modes of high density condense at the transition, signaling restoration of lattice symmetry. These unconventional features are consistent with "deconfined quantum criticality".

Problems related to quantum criticality in quantum spin systems are of both fundamental and practical importance [1]. Numerous materials, such as Mott insulators, exhibit either antiferromagnetic (Néel) order or quantum disordered (spin gapped) ground state depending on the distribution of Heisenberg exchange couplings and geometry. External perturbations (such as doping or frustration) can also cause quantum transitions between these phases. It is well understood that the quantum transition between a quantum disordered and a Néel phase is in the $O(3)$ universality class [1], where a triplet state condenses at the quantum critical point (QCP).

A recent exciting development in our theoretical understanding of QCPs originated from the proposal that if the quantum disordered (QD) phase spontaneously breaks lattice symmetries (*e.g.* is characterized by spontaneous dimer order), and the transition is of second order, then exactly at the QCP spinon deconfinement occurs, *i.e.* the excitations are fractionalized [2]. It is assumed that the Hamiltonian itself does not break the lattice symmetries (*i.e.* does not have "trivial" dimer order caused by some exchanges being stronger than the others). We use the terms "dimer order" and "valence bond solid (VBS) order" interchangeably. It is expected that the dimer order vanishes exactly at the point where Néel order appears, *i.e.* there is no coexistence between the two phases. Deconfinement thus is intimately related to disappearance of VBS order; indeed if the latter persisted in the Néel phase it would be impossible to isolate a spinon, as "pairing" would always take place. Spontaneous VBS order driven by frustration has been a common theme in quantum antiferromagnetism [3], although its presence and the nature of criticality in specific models, such as the 2D square-lattice frustrated Heisenberg antiferromagnet, is still somewhat controversial [4]. Unbiased numerical approaches, most notably the Quantum Monte Carlo (QMC) method, cannot be used to analyze frustrated spin models.

In a very recent study, the QMC method was applied to a four-spin exchange quantum spin model without frustration, which was shown to exhibit VBS order and a magnetically ordered phase with a deconfined QCP sep-
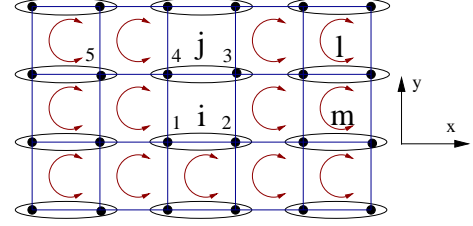

FIG. 1: (Color online) Dimer pattern in the quantum disordered (VBS) phase, $K/J > (K/J)_c$.

arating them [5]. It is the objective of the present work to study this model by approaching the quantum transition from the VBS phase. Our approach uses as a starting point a symmetry broken state (*i.e.* one out of four degenerate VBS configurations), and we thus must search for signatures that the system attempts to restore the lattice symmetry at the QCP. Even though full restoration is impossible within the present framework, we find a QCP characterized by condensation of triplet modes of high density; this is the opposite of the conventional situation when the condensing particles are in the dilute Bose gas limit. The high density itself is due to the presence of a singlet mode that condenses at the QCP, and reflects the strong fluctuations of the background dimer order. The above effects translate into a tendency towards vanishing of the VBS order, which provides evidence of the unconventional nature of the quantum phase transition in this model.

The model under consideration is

$$H = J \sum_{\langle i,j \rangle} \mathbf{S}_i . \mathbf{S}_j - K \sum_{i,j,k,l} (\mathbf{S}_i \cdot \mathbf{S}_j)(\mathbf{S}_k \cdot \mathbf{S}_l), \quad (1)$$

where $J > 0, K > 0$, and all spins are $S = 1/2$. Consider the numbers 1,2,3,4 in Fig. 1. The summation in the four-spin term is over indexes $(i,j) = (1,2), (k,l) = (3,4)$ and $(i,j) = (1,4), (k,l) = (2,3)$ on a given plaquette, and then summation is made over all plaquettes. The range of parameters explored in [5] is $K/J \leq 2$, with a QCP in the interval $1.67 \lesssim (K/J)_c \lesssim 2$. For simplicity, we will use $(K/J)_c \approx 2$. The dimerization pattern is proposed to

be of the "columnar" type, as shown in Fig. 1. Four such configurations exist. We will assume a configuration of this type, will show that it is stable at $K/J \gg 1$, and will then search for an instability towards the Néel state as K/J decreases [6].

Mean-field treatment. $-$ We start by rewriting Eq. (1) in the the bond-operator representation [7], where on a dimer $\mathbf{i}$, the two spins forming it are expressed as: $S_{1,2}^{\alpha} = \frac{1}{2}(\pm s_{\mathbf{i}}^{\dagger} t_{\mathbf{i}\alpha} \pm t_{\mathbf{i}\alpha}^{\dagger} s_{\mathbf{i}} - i\epsilon_{\alpha\beta\gamma} t_{\mathbf{i}\beta}^{\dagger} t_{\mathbf{i}\gamma})$, and $s_{\mathbf{i}}^{\dagger}, t_{\mathbf{i}\alpha}^{\dagger}, \alpha = x, y, z$ create a singlet and triplet of states. We refer to the triplet (S=1) quasiparticle, $t_{\mathbf{i}\alpha}^{\dagger}$, as "triplon". The bold indexes $\mathbf{i}, \mathbf{j}, \mathbf{m}, \mathbf{l}$ now label dimers. Summation over repeated Greek indexes is assumed. The hard-core constraint, $s_{\mathbf{i}}^{\dagger} s_{\mathbf{i}} + t_{\mathbf{i}\alpha}^{\dagger} t_{\mathbf{i}\alpha} = 1$, must be enforced on every site, which at the mean-field (MF) level can be done by introducing a term in the Hamiltonian, $-\mu \sum_{\mathbf{i}} (s^2 + t_{\mathbf{i}\alpha}^{\dagger} t_{\mathbf{i}\alpha} - 1)$. Then μ and the (condensed) singlet amplitude $s \equiv \langle s_{\mathbf{i}} \rangle$, are determined by the MF equations [7]. We obtain at the quadratic level, in momentum representation:

$$H_2 = \sum_{\mathbf{k},\alpha} \left\{ A_{\mathbf{k}} t_{\mathbf{k}\alpha}^{\dagger} t_{\mathbf{k}\alpha} + \frac{B_{\mathbf{k}}}{2} \left(t_{\mathbf{k}\alpha}^{\dagger} t_{-\mathbf{k}\alpha}^{\dagger} + \text{h.c.} \right) \right\} \quad (2)$$

$$\begin{aligned}
A_{\mathbf{k}} &= J/4 - \mu + s^2(\xi_{\mathbf{k}}^{-} + K/2) + s^4 \Sigma(\mathbf{k}) , \\
B_{\mathbf{k}} &= s^2 \xi_{\mathbf{k}}^{+} + s^4 \Sigma(\mathbf{k}) , \\
\xi_{\mathbf{k}}^{\pm} &= -(J/2) \cos k_x + (J \pm K/4) \cos k_y .
\end{aligned} \quad (3)$$

The four-spin interaction from (1) acting between two dimers (*e.g.* $\mathbf{i}, \mathbf{j}$ in Fig. 1) contributes to the "on-site" gap and hopping ($\xi_{\mathbf{k}}^{-}$) via $A_{\mathbf{k}}$, as well as to the quantum fluctuations $B_{\mathbf{k}}$. The part involving four dimers has been split in a mean-field fashion, leading to the Hartree-Fock self-energy

$$-\Sigma(\mathbf{k})/K = 2\Sigma_x \cos k_x + 2\Sigma_y \cos k_y + \Sigma_{xy} \cos k_x \cos k_y, \quad (4)$$

with $\Sigma_x = (1/3) \sum_{\alpha} \langle t_{\mathbf{i}\alpha}^{\dagger} t_{\mathbf{m}\alpha} + t_{\mathbf{i}\alpha}^{\dagger} t_{\mathbf{m}\alpha}^{\dagger} \rangle$, where $\mathbf{i}, \mathbf{m}$ are neighboring dimers in the x direction (Fig. 1), and similarly for the y and the diagonal contributions. The triplon dispersion is $\omega(\mathbf{k}) = \sqrt{A_{\mathbf{k}}^2 - B_{\mathbf{k}}^2}$, and has a minimum at the Néel ordering wave-vector $\mathbf{k}_{AF} = (0, \pi)$ (since we work on a dimerized lattice). The ground state energy is then easily computed via $E_{GS} = E_0 + \langle H_2 \rangle$, with $E_0/N = (-3/4)(Js^2 + Ks^4) + \mu(-s^2 + 1) + 3Ks^4(\Sigma_x^2 + \Sigma_y^2 + (1/2)\Sigma_{xy}^2)$, and the mean-field equations require a numerical minimization with respect to the parameters $\{\mu, s, \Sigma_x, \Sigma_y, \Sigma_{xy}\}$. This amounts to self-consistent Hartree-Fock for $\Sigma(\mathbf{k})$. The result for the triplon gap $\Delta = \omega(\mathbf{k}_{AF})$ is presented in Fig. 2 (black curve).

The MF result $(K/J)_c \approx 0.6$ substantially underestimates the location of the critical point. Interestingly, if one solves the MF equations ignoring both the hard core and the $\Sigma(\mathbf{k})$, one finds $(K/J)_c = 1$. Physically, in the full MF, the hard core contribution increases the gap (and hence the stability of the dimer phase) while at
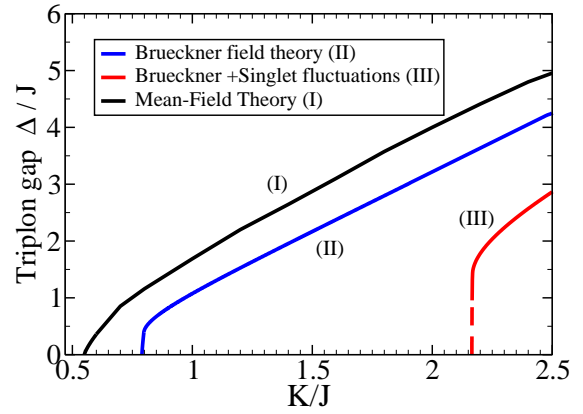

FIG. 2: (Color online) Triplon excitation gap $\Delta = \omega(\mathbf{k}_{AF})$ in various approximations. The point $\Delta \to 0$ corresponds to transition to the Néel phase.

the same time suppressing the antiferromagnetic fluctuations (which favor the Néel state). Hence it is crucial to go beyond mean-field theory.

Beyond mean-field. Dilute triplon gas approximation. $-$ A more accurate treatment of fluctuations is possible by taking into account the hard-core constraint beyond mean-field. One can set the singlet amplitude $s = 1$ in the previous formulas, but introduce an infinite on-site repulsion between the triplons, $U \sum_{\mathbf{i},\alpha\beta} t_{\alpha\mathbf{i}}^{\dagger} t_{\beta\mathbf{i}}^{\dagger} t_{\beta\mathbf{i}} t_{\alpha\mathbf{i}}$, $U \to \infty$. As long as the triplon density (determined by the quantum fluctuations) is low, an infinite repulsion corresponds to a finite scattering amplitude between excitations and can be calculated by resumming ladder diagrams for the scattering vertex [8]. This leads to the effective triplon-triplon vertex $\Gamma(\mathbf{k}, \omega)$ [9]:

$$\Gamma^{-1}(\mathbf{k}, \omega) = \sum_{\mathbf{q}} \frac{u_{\mathbf{q}}^2 u_{\mathbf{k}-\mathbf{q}}^2}{\omega(\mathbf{q}) + \omega(\mathbf{k}-\mathbf{q}) - \omega} + \left\{ \begin{array}{c} u \to v \\ \omega \to -\omega \end{array} \right\}, \quad (5)$$

which in turn affects the triplon dispersion via (what we call) the Brueckner self-energy:

$$\Sigma_B(\mathbf{k}, \omega) = 4 \sum_{\mathbf{q}} v_{\mathbf{q}}^2 \Gamma(\mathbf{k} + \mathbf{q}, \omega - \omega(\mathbf{q})). \quad (6)$$

The corresponding parameters in the quadratic Hamiltonian (2) in this case are

$$\begin{aligned}
A_{\mathbf{k}} &= J + 2K(1 - 4n_t/3) + \xi_{\mathbf{k}}^{-} + \Sigma(\mathbf{k}) + \Sigma_B(\mathbf{k}, 0) \\
B_{\mathbf{k}} &= \xi_{\mathbf{k}}^{+} + \Sigma(\mathbf{k}).
\end{aligned} \quad (7)$$

The Bogolubov coefficients are defined in the usual way $u_{\mathbf{k}}^2 = 1/2 + A_{\mathbf{k}}/(2\omega(\mathbf{k})) = 1 + v_{\mathbf{k}}^2$. The various terms in $\Sigma(\mathbf{k})$ can be expressed through them: for example $\Sigma_x = \sum_{\mathbf{k}} (v_{\mathbf{k}}^2 + v_{\mathbf{k}} u_{\mathbf{k}}) \cos k_x$, and so on. The density of triplons is $n_t = \langle t_{\mathbf{i}\alpha}^{\dagger} t_{\mathbf{i}\alpha} \rangle = 3 \sum_{\mathbf{k}} v_{\mathbf{k}}^2$. In addition, the renormalization of the quasiparticle residue,
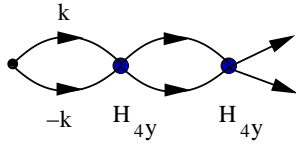
FIG. 3: Renormalization of quantum fluctuations by resummation of a ladder series, with (8) at the vertices.

$Z_{\mathbf{k}}^{-1} = 1 - \partial \Sigma_B(\mathbf{k}, 0)/\partial \omega$, implies the replacement $u_{\mathbf{k}} \to \sqrt{Z_{\mathbf{k}}} u_{\mathbf{k}}$, $v_{\mathbf{k}} \to \sqrt{Z_{\mathbf{k}}} v_{\mathbf{k}}$ in all the formulas [9], and the renormalized spectrum $\omega(\mathbf{k}) = Z_{\mathbf{k}} \sqrt{A_{\mathbf{k}}^2 - B_{\mathbf{k}}^2}$.

An iterative numerical evaluation of the spectrum using the above equations, which amounts to solution of the Dyson equation, leads to the result in Fig. 2 (blue curve). The diagram resummations appear to be well justified since the quasiparticle density $n_t < 0.1$. The resulting critical point is still in the "weak-coupling" regime $K/J < 1$, with about 100% deviation from the QMC result $((K/J)_c \approx 2)$.

Strong fluctuations in the singlet background. QCP beyond the dilute triplon gas approximation. — It is clear that "non-perturbative" effects are responsible for driving the QCP towards the "strong-coupling" region $K/J \sim 2$. To proceed we make two improvements to the previous low-density, weak-coupling theory.

First, we take into account fluctuations in the singlet background, *i.e.* the manifold on which the triplons are built and interact. The main effect originates from the action of the four-spin K-term from (1) on two dimers, *e.g.* $\mathbf{i}, \mathbf{j}$ in Fig. 1. Part of this action has led to the on-site gap $2K$ in (7), favoring dimerization. However, a strong attraction between the two dimers is also present, since the K-term is symmetric with respect to the index pair exchange $(1,2)(3,4) \leftrightarrow (1,4)(2,3)$, leading to a "plaquettization" tendency as well. In the triplon language this is manifested by formation of bound states of two triplons, due to their nearest-neighbor interactions

$$
\begin{aligned}
H_{4,y} &= \sum_{\langle \mathbf{i}, \mathbf{j} \rangle_y, \alpha\beta} \Big\{ \gamma_1 t_{\alpha \mathbf{i}}^\dagger t_{\beta \mathbf{j}}^\dagger t_{\beta \mathbf{i}} t_{\alpha \mathbf{j}} + \gamma_2 t_{\alpha \mathbf{i}}^\dagger t_{\alpha \mathbf{j}}^\dagger t_{\beta \mathbf{i}} t_{\beta \mathbf{j}} \\
&\quad + \gamma_3 t_{\alpha \mathbf{i}}^\dagger t_{\beta \mathbf{j}}^\dagger t_{\alpha \mathbf{i}} t_{\beta \mathbf{j}} \Big\}, \\
\gamma_1 &= -K/8 + J/2, \; \gamma_2 = -K/8 - J/2, \; \gamma_3 = -5K/4.
\end{aligned} \tag{8}
$$

We also checked that on the perturbative (Hartree-Fock) level, the effect of this term on equations (3) and (7) was negligible (and we do not write it explicitly).

An intuitive way of taking into account the effect of two-triplon bound states (with total spin S=0) on the one-triplon spectrum, is to work in the "local" approximation. This means effectively neglecting the triplon dispersion and directly evaluating the ladder series that renormalizes the quantum fluctuation term $B_{\mathbf{k}}$ in (2), corresponding to emission of a pair of triplons with zero
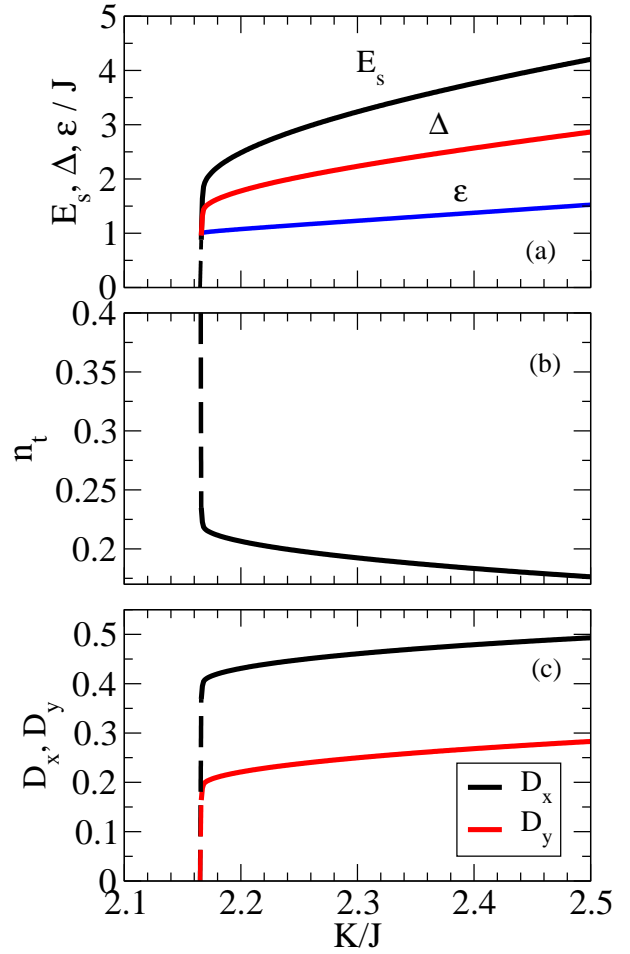

FIG. 4: (Color online) (a.) Singlet bound state energy E_s (black), binding energy $\epsilon = 2\Delta - E_s$ (blue), and the triplon gap Δ (red). (b.) Triplon density n_t. (c.) Dimer order parameters. Dashed parts of the lines represent points corresponding to rapid growth of the quasiparticle density.

total momentum. This is illustrated in Fig. 3, with the result

$$
B_{\mathbf{k}} \to -\frac{J}{2} \cos k_x + \frac{J + K/4}{1 - \frac{|\gamma|}{|\Delta E|}} \cos k_y + \Sigma(\mathbf{k}),
$$

$$
\gamma \equiv \gamma_1 + 3\gamma_2 + \gamma_3 = -J - 7K/4, \tag{9}
$$

where γ is the effective attraction of two triplons with total $S = 0$, and $\Delta E = 2J + 11K/4$ is the energy of two (non-interacting) triplons on adjacent sites. This calculation is justified for $K/J \gg 1$ and leads to an increase of the quantum fluctuations, and from there to almost doubling of the triplon density n_t (see Fig. 4 below). It contributes significantly to the shift of the QCP.

We can go beyond the "local" approximation by solving the Bethe-Salpeter equation for the bound state, formed due to the attraction (8), and taking into account the full triplon dispersion. The equation for the singlet

bound state energy $E_s(\mathbf{Q})$, corresponding to total pair momentum $\mathbf{Q}$ is

$$1 = 2\gamma \sum_{\mathbf{q}} \frac{u_{\mathbf{q}}^4 \cos^2 q_y}{E_s(\mathbf{Q}) - \omega(\mathbf{Q}/2 + \mathbf{q}) - \omega(\mathbf{Q}/2 - \mathbf{q})}. \quad (10)$$

Here we have, for simplicity, written only the main contribution to pairing (Eq. (8)) in the limit $K/J \gg 1$, and have neglected the on-site repulsion (which leads to slightly diminished pairing), as well as small pairing due to the exchange J from dimers in the x-direction on Fig. 1. It is easily seen that the lowest energy corresponds to $\mathbf{Q} = 0$; we define $E_s \equiv E_s(\mathbf{Q} = 0)$. The binding energy is $\epsilon = 2\Delta - E_s$, where Δ is the one-particle gap. The bound state wave-function corresponding to E_s is $|\Psi\rangle = \sum_{\alpha, \mathbf{i}, \mathbf{j}, q_y} \Psi_{q_y} e^{iq_y(\mathbf{i}-\mathbf{j})} t_{\alpha\mathbf{i}}^\dagger t_{\alpha\mathbf{j}}^\dagger |0\rangle$.

Second, we have made subtle changes to the resummation procedure concerning the quasiparticle renormalization Z, based on both formal and physical grounds. On the one hand it is clear that in the Brueckner approximation (Eq. (6)), where the self energy is linear in the density ($\Sigma_B \propto n_t$), the dependence of the vertex Γ^{-1} on density is beyond the accuracy of the calculation, meaning one can put $u_{\mathbf{q}} = 1, v_{\mathbf{q}} = 0$ in (5), instead of determining them self-consistently. This leads to a decreased influence of the hard-core Σ_B (which favors the dimer state) on the Hartree-Fock self-energy $\Sigma(\mathbf{k})$ from (4) (which favors the Néel state). It is indeed the mutual interplay between $\Sigma_B > 0$ and $\Sigma(\mathbf{k}) < 0$, that determines the exact location of the QCP in the course of the Dyson's equation iterative solution. While in the "weak-coupling" regime $K/J < 1$, Σ_B always dominates, in the "strong-coupling" region $K/J > 2$, $\Sigma(\mathbf{k})$ starts playing a significant role, since parametrically $\Sigma \propto Kn_t$. It is physically consistent that in the region where singlet fluctuations in the dimer background are strong, the hard-core effect is less important, i.e. in effect the kinematic hard-core constraint is "relaxed". We also observe that in typical models with QCP driven by explicit dimerization, such as the bilayer model, the described difference in approximation schemes makes a very small difference on the location of the QCP [10], since those models are always in the "weak-coupling" regime, dominated by the hard-core repulsion of excitations on a non-fluctuating dimer configuration.

Our results are summarized in Fig. 4 and Fig. 2 (red line) for the gap. The critical point is shifted towards $(K/J)_c \approx 2.16$ (in good agreement with QMC data), with a very strong increase of the density towards K_c. This translates into a decrease of the dimer order, as measured by the two dimer order parameters that we compute from: $D_x = |\langle \mathbf{S}_3 \cdot \mathbf{S}_4 \rangle - \langle \mathbf{S}_5 \cdot \mathbf{S}_4 \rangle| = |-\frac{3}{4} + n_t + \frac{3}{4}\Sigma_x|$, $D_y = |\langle \mathbf{S}_3 \cdot \mathbf{S}_4 \rangle - \langle \mathbf{S}_1 \cdot \mathbf{S}_4 \rangle| = |-\frac{3}{4} + n_t - \frac{3}{4}\Sigma_y|$. The spins are labeled as in Fig. 1. The singlet bound state energy $E_s(0)$ also tends towards zero at the QCP, with the corresponding binding energy remaining quite large

$\epsilon/J \approx 1$. All these effects point towards a tendency of the system to restore the lattice symmetry, although it is certainly clear that as the critical point is approached, our approximation scheme (low density of quasiparticles) breaks down (dashed lines on figures). We should point out that the sharpness of variation near K_c is not due to divergence in any of the self-energies but is a result of rapid cancellation at high orders (i.e. iterations in the Dyson equation). In fact cutting off our iterative procedure at finite order gives a smooth curve, suggesting that additional classes of diagrams become important (although in practice their classification is an unsurmountable task). The merger of singlet and triplet modes, which we find near the QCP, reflects a tendency towards quasiparticle fractionalization (spinon deconfinement) and is also found in the 1D Heisenberg chain with frustration [11], where spinons are always deconfined.

In conclusion, we have shown that the QCP between the Néel and the dimer state in the model (1) is of unconventional nature, characterized by the presence of both triplet and singlet low-energy modes. Near the QCP, whose location $((K/J)_c \approx 2)$ we find in good agreement with recent QMC studies, the system exhibits: (1.) Strong rise of the triplon excitation density, due to increased quantum fluctuations, (2.) Corresponding strong decrease of the dimer order, (3.) Vanishing of a singlet energy scale, related to the destruction of the dimer "columns" in Fig. 1. The above effects are all related and influence strongly one another, ultimately meaning that the QCP reflects strong fluctuations and can not be described in a mean-field theory framework. Our study thus provides additional evidence that the quantum transition reflects "deconfined criticality" and liberation of spinons, of which the present model is believed to be the only example so far.

[1] S. Sachdev, *Quantum Phase Transitions* (Cambridge University Press, Cambridge, 1999).

[2] T. Senthil *et al.*, Science **303**, 1490 (2004); T. Senthil *et al.*, Phys. Rev. B **70**, 144407 (2004).

[3] S. Sachdev and N. Read, Int. J. Mod. Phys. B **5**, 219 (1991).

[4] R. R. P. Singh *et al.*, Phys. Rev. B **60**, 7278 (1999); L. Capriotti *et al.*, Phys. Rev. Lett. **87**, 097201 (2001); M. Mambrini *et al.*, Phys. Rev. B **74**, 144422 (2006).

[5] A. W. Sandvik, arXiv:cond-mat/0611343 (2006).

[6] The possibility of four-spin exchange induced dimerization has been discussed in the context of the full ring exchange, of which the interaction (1) is part; see e.g. A. Läuchli *et al.*, Phys. Rev. Lett. **95**, 137206 (2005).

[7] S. Sachdev and R. N. Bhatt, Phys. Rev. B **41**, 9323 (1990).

[8] A. L. Fetter and J. D. Walecka, *Quantum Theory of Many-Particle Systems* (Dover Publications, Mineola, NY, 2003).

[9] V. N. Kotov *et al.*, Phys. Rev. Lett. **80**, 5790 (1998).

[10] P. V. Shevchenko, A. W. Sandvik, and O. P. Sushkov, Phys. Rev. B **61**, 3475 (2000).

[11] W. H. Zheng *et al.*, Phys. Rev. B **63**, 144411 (2001); *ibid.* **63**, 144410 (2001).